Journal of Engineering Mathematics (Springer)

Impact factor = 1.434

Editor in chief: Prof. O. K. Matar, Imperial College London.

Accepted February 16th 2021

TAYLOR DISPERSION IN NON-DARCY POROUS MEDIA WITH BULK CHEMICAL REACTION: *A MODEL FOR DRUG TRANSPORT IN IMPEDED BLOOD VESSELS*

Ashis Kumar Roy[a]*, O. Anwar Bég[b], Apu Kumar Saha[c] and J.V. Ramana Murthy[d]

[a]Department of Science & Humanities, Tripura Institute of Technology, Agartala, Tripura-799009, ***India***

[b]Multi-Physical Engineering Sciences Group, Mechanical Engineering Department, School of Science, Engineering and Environment (SEE), University of Salford, Manchester, ***UK.***

[c]Department of Mathematics, National Institute of Technology Agartala, Tripura-799046, ***India.***

[d]Department of Mathematics, National Institute of Technology Warangal, Telangana-506004, ***India.***

****Corresponding Author: Email:*** *rk.ashis10@gmail.com*

ABSTRACT

The present article discusses the solute transport process in unsteady laminar blood flow through a non-Darcy porous medium, as a model for drug movement in blood vessels containing deposits. The Darcy-Brinkman-Forchheimer drag force formulation is adopted to mimic a sparsely packed porous domain, and the vessel is approximated as an impermeable cylindrical conduit. The conservation equations are implemented in an axisymmetric system (R, Z) *with suitable boundary conditions, assuming constant tortuosity and porosity of the medium. Newtonian flow is assumed, which is physically realistic for large vessels at high shear rates. The velocity field is expanded asymptotically, and the concentration field decomposed. Advection and dispersion coefficient expressions are rigorously derived. Extensive visualization of the influence of effective Péclet number, Forchheimer number, reaction parameter on velocity, asymptotic dispersion coefficient, mean concentration, and transverse concentration at different axial locations and times are provided. Increasing reaction parameter and Forchheimer number both decrease the dispersion coefficient, although the latter exhibits a linear decay. The maximum mean concentration is enhanced with greater Forchheimer numbers, although the centre of the solute cloud is displaced in the backward direction. Peak mean concentration is suppressed with the reaction parameter, although the centroid of the solute cloud remains unchanged. Peak mean concentration deteriorates over time since the dispersion process is largely controlled by diffusion at the large time, and therefore the breakthrough curve is more dispersed. A similar trend is computed with increasing Péclet number (large Péclet numbers imply diffusion-controlled transport). The computations provide some insight into a drug (pharmacological agents) reacting linearly with blood.*

KEYWORDS*: Taylor dispersion, Forchheimer coefficient, Bulk flow reaction; porous media; Péclet number; pharmaco-dynamics; axial and radial diffusion.*

1.INTRODUCTION

Solute transport in porous media continues to mobilize substantial attention of researchers throughout the globe due to its diverse applications in several branches of technology and environmental sciences. These include contaminant transport (Sahimi, 2011), geological carbon storage (Popova et al., 2012; Szulczewski et al., 2012), and environmental protection (Wang and Chen, 2015; Wang et al., 2013, 2015) etc. Furthermore, in certain hemodynamic scenarios e.g., the molecular reaction of oxygen in the vasculature, solute transport is important. This can lead to, for example, endothelial dysfunction in chronic flow overload (Taniyama and Griendling, 2003; Touyz and Schirin, 2004). The transport of solute, whether in biological or other systems, is the result of *advection and molecular diffusion mechanisms*. *Advection* is responsible for carrying the centre of mass of an injected solute band, whereas *molecular diffusion* helps to spread the solute from a high concentration zone to a low concentration zone. For uniform velocity, the concentration of the dissolved band is low on both sides, which assists in molecular diffusion towards the axial direction, a phenomenon often termed *axial dispersion*. However, for non-uniform velocity profiles, a radial concentration gradient is observed, which induces radial diffusion. Taylor (1953) first studied this phenomenon for laminar flow through a capillary by neglecting axial diffusion, and thereafter the mechanism of solute dispersion in a shear flow has popularly been termed as *Taylor dispersion*. Even in the case of flow through porous media, the tracer material is dispersed by molecular diffusion and convective or mechanical diffusion. This convective diffusion in porous media is due to the irregular flow pattern, and the source of this irregular flow pattern is a complex geometric structure of the permeable medium. Therefore, the hydrodynamic dispersion in porous media is highly complex, microscopic, and consequently a challenge to simulate mathematically. The best way to describe this complicated process is to formulate the

problem by considering a molecular picture through mathematical simplification such as *statistical averages*. The Slattery-Whitaker theorem is one of the important mathematical aspects in deriving the fluid's average properties through porous media. This theorem was independently discovered by both Slattery Slattery (1967) and Whitaker (1967) in the context of chemical engineering fluid dynamics at the same time. In fact, these averages are statistical averages of physical quantities taken over some representative volume of the system.

The seepage velocity generally utilized in the above studies is governed by Darcy's law (Darcy, 1856), an empirical law which explicitly states that the flow rate is proportional to the applied pressure gradient in steady flow through porous media. In modern notation, this is expressed as $\bar{q} = -\mu^{-1}\mathbf{K}\nabla P$, where, $\bar{q}$ is the seepage or Darcy velocity and $\mathbf{K}$ is the permeability tensor. For the case of isotropic porous media (i.e. a single permeability in all directions), this law can be modified as $\nabla P = -(\mu / K)\bar{q}$. The Darcy law is relevant for a tightly packed porous medium having very low permeability that quantifies only the frictional force applied on a fluid element by the solid particles instead of usual viscous force. Beavers et al. (1970) experimentally observed the presence of shear inside the porous medium, near the boundaries. The Darcy equation failed to predict the presence of such a boundary region as the equation does not incorporate the macroscopic shear term. Tam (1969) and Slattery (1970) modified Darcy's equation by including the shear term in the form

$$\nabla P = \mu'\nabla^2\bar{q} - \frac{\mu}{K}\bar{q}. \tag{1}$$

Here μ' is the effective viscosity, which is a function porosity ϕ of the porous medium. The Eq. (1) most acceptable governing equation for an incompressible creeping flow of

a Newtonian fluid in an anisotropic, homogeneous porous medium, originally proposed by Dutch petroleum engineer Brinkman (1949 a, b, c). A complete statistical interpretation of the Eq. (1) was subsequently given by Saman (1971) and Lundgren (1972). The Brinkman model is true for a loosely packed fluid-saturated porous medium where there is a large vacuum (space) for a fluid to flow so that the distortion of velocity increase the usual viscous shear force. However, in a variety of realistic situations under which the porosity of the porous medium is close to unity, the flow of fluid is curvilinear, and curvature of the path induces the inertia effect. The substantially increasing inertia force as compared to the viscous force increases the drag more rapidly with velocity. Lapwood (1948) gave a mathematical form incorporating the convective inertial term, thereby extending Eq. (1) to:

$$\frac{\rho}{\phi^2}\nabla(\bar{q}\cdot\bar{q}) = -\nabla P + \mu'\nabla^2\bar{q} - \frac{\mu}{K}\bar{q}. \tag{2}$$

Equation (2) does not consider the *unsteady* nature of the flow, and for this reason, the Eq. (2) is further modified by including local acceleration term as follows (Nield and Bejan, 2013; Vafai and Kim, 1995):

$$\rho\left[\frac{1}{\phi}\frac{\partial\bar{q}}{\partial t} + \frac{1}{\phi^2}\nabla(\bar{q}\cdot\bar{q})\right] = -\nabla P + \mu'\nabla^2\bar{q} - \frac{\mu}{K}\bar{q}. \tag{3}$$

In Darcy's law, the seepage velocity $\bar{q}$ is linear and holds when $\bar{q}$ is sufficiently small (Reynolds number order of pore size). As $\bar{q}$ increases Reynolds number is within the range $1-10$; clearly this transition, not one from laminar to turbulent. However, in this regime of Reynolds number, a change from linear drag to non-linear drag is observed. By including the quadratic drag in the system, the above Eq. (3) becomes:

$$\rho\left[\frac{1}{\phi}\frac{\partial \overline{q}}{\partial t}+\frac{1}{\phi^2}\nabla(\overline{q}\cdot\overline{q})\right]=-\nabla P+\mu'\nabla^2\overline{q}-\frac{\mu}{K}\overline{q}-\frac{\rho C_f}{\sqrt{K}}|\overline{q}|\overline{q} \quad (4)$$

Equation (4) is known as the Darcy-Lapwood-Brinkman-Forchheimer model, where C_f designates the quadratic (Forchheimer) drag coefficient. As noted earlier, solute dispersion features in a number of biophysical transport phenomena. A blood vessel in the human body is one of the best examples of porous media in a biological system due to the presence of fatty plug in the lumen of the blood artery. Blood flow modelling (and indeed other physiological systems) with porous media effects have therefore stimulated considerable attention in modern biofluid dynamics. These investigations have featured both Newtonian and non-Newtonian models and deployed both analytical and numerical methods. Dash et al. (1996) used the Darcy-Brinkman model to study viscoplastic (yield stress) blood flow in an isotropic porous medium through a tube. Tripathi and Bég (2012) presented homotopy power series solutions for viscoelastic blood transport under peristaltic waves with hydrodynamic slip in generalized Darcy-Brinkman porous media. Ravi Kiran et al. (2017) derived exact solutions for hydrodynamic dispersion in micropolar gastric flow with homogenous chemical reaction. Bég et al. (2007) used a Darcy-Forchheimer-Brinkman model, variational finite elements and finite difference algorithms to analyze the biomagnetic micropolar convective blood flow in porous media. Chapelle et al. (2009) used higher-order penalty finite element algorithms with a poro-elastic Darcy model to compute the blood flow and vessel deformation in cardiac perfusion. Rashidi et al. (2010) employed a differential transform algorithm to study the magnetized micropolar blood flow and heat transfer in Darcy-Brinkman-Forchheimer porous media, noting the significant deceleration associated with higher Forchheimer drag effects. Bég et al. (2013) applied Liao's homotopy method to derive analytical solutions for two-phase blood flow and thermal convection in a Darcy-Forchheimer-

porous medium with Stokes number effects. The Darcy-Brinkman-Forchheimer model has also been deployed by Bég et al. (2012) (on pulsating blood flow with a pharmacological mass transfer under a magnetic field). The Darcy-Brinkman model has been implemented by Tripathi and Bég (2012) (on annular polar hemodynamic peristaltic microvascular flow in permeable media) and Tripathi and Bég (2012) (on unsteady propulsion of gastric viscoelastic suspensions in intestinal conduits containing permeable media.

Generally, the above studies have ignored reactive hydrodynamic dispersion in blood flows through porous media. Such flows, as noted earlier, have direct relevance to oxygen transport in hemodynamics and also controlled drug release in pharmacodynamics (Weiser and Saltzman, 2014). It is well known that pharmaco-kinetic models furnish very limited insight into the fate of drugs released in blood flows. The dispersion process of pharmaceuticals is regulated locally by physiological transport principles, which are particular to the anatomic site and can significantly impact the agent release rate from the controlled release device as well as its fate in the local tissues. As such, fluid dynamic dispersion models (pharmaco-dynamic) offer a more comprehensive foundation for analysing such phenomena than conventional pharmaco-kinetic models deployed in medicine. They facilitate the bioengineers to investigate the local drug (reactive agent) transport released from the controlled release device and during migration through the local tissues and deposits (porous media), allowing a deeper understanding of the significance of local drug delivery constraints (Peppas and Sahlin, 1989; Saltzman, 2001). The current work may also be of pertinence in nano-drug delivery systems (Dubey et al., 2020; Tripathi et al., 2020b) and hypercholesterolemia (Ohara et al., 1993) and also redox reaction mechanisms in blood vessels (Mueller et al., 2005). Motivated by these applications, the current study has devolved a comprehensive mathematical model for

unsteady blood flow through a cylindrical vessel containing porous media in which a fully miscible and chemically active species (pharmacological agent) is injected. The porous medium is governed by the Darcy-Brinkman-Forchheimer model, and the Newtonian model is deployed, which is valid for large vessels at high shear rates. The conservation equations are formulated in an axisymmetric coordinate system (R, Z) with appropriate boundary conditions, assuming constant tortuosity and porosity of the medium. Both axial and radial diffusion are considered. The general convective diffusion equation is rendered dimensionless with appropriate transformations and solved using a regular perturbation method taking the perturbation parameter as $1/\sqrt{\mathrm{Da}}$ where Da is the Darcy number (dimensionless permeability parameter). The velocity field is expanded asymptotically, and the concentration field decomposed. Advection and dispersion coefficient expressions are rigorously derived. Comprehensive graphs are displayed to explore the influence of effective Péclet number, Forchheimer number and reaction parameter on velocity, asymptotic dispersion coefficient, mean concentration, and also transverse concentration at different axial locations and times.

2. MATHEMATICAL FORMULATION

Consider the transport of a reactive solute (e.g., pharmacological agent, oxygen, etc.) in a cylindrical rigid, impermeable walled-blood vessel containing sparsely packed porous media as depicted in Fig. 1. The porous medium is saturated with blood and is assumed to be non-deformable i.e.; elastic matrix effects are negated. In view of this, we recall following (Chen and Wu, 2012; Chen and Zeng, 2009; Wang and Chen, 2015; Wang et al., 2013) the *general convective diffusion equation in the average phase scale* as:

$$\frac{\partial C}{\partial t}+\frac{\bar{q}}{\phi}\cdot \text{ grad } C=\nabla\cdot(k\lambda\nabla C)+\frac{k}{\phi}\nabla\cdot(\mathbf{D}\cdot\nabla C)-\phi\beta C. \tag{5}$$

The variables and parameters are used in the above equations are defined in **Table 1** below.

Table 1. List of variable and parameters

Symbols	**Name**	**Unit**
t	Time	s
$\bar{q}$	Superficial velocity	$\mathrm{m\ s^{-1}}$
K	Permeability (hydraulic conductivity)	$\mathrm{m^2}$
ϕ	Porosity	Dimensionless
C	Solute concentration	$\mathrm{kg\ m^{-3}}$
λ	Concentration diffusivity	$\mathrm{m^2\ s^{-1}}$
k	Tortuosity	Dimensionless
D	Concentration dispersion tensor	$\mathrm{m^2\ s^{-1}}$
β	Bulk flow reaction rate	$\mathrm{s^{-1}}$

Consider a tracer transport in a fully developed unidirectional (i.e., $\bar{q} = (0,0,U)$), steady blood (assumed to be Newtonian) flow with constant ϕ, λ, k and **D** through a blood vessel (a circular tube of radius a). The blood vessel is assumed to be a sparsely packed isotropic porous medium and $\mu = \mu'$. With this assumption, the momentum Eq. (4) is then reduced to:

$$\frac{\nu}{R}\frac{\partial}{\partial R}\left(R\frac{\partial U}{\partial R}\right) - \frac{\nu}{K}U - \frac{C_f}{\sqrt{K}}U^2 - \frac{1}{\rho}\frac{\partial p}{\partial Z} = 0,\ \ 0 < R < a. \tag{6}$$

Here, $\nu = \mu / \rho$ is the kinematic viscosity, and the axial pressure gradient $\partial p / \partial Z$ is assumed to constant. The conditions at the boundary (vessel wall) are imposed as:

$$\left.\begin{aligned} U < \infty \quad &\text{at} \quad R = 0, \\ U = 0 \quad &\text{at} \quad R = a. \end{aligned}\right\} \tag{7}$$

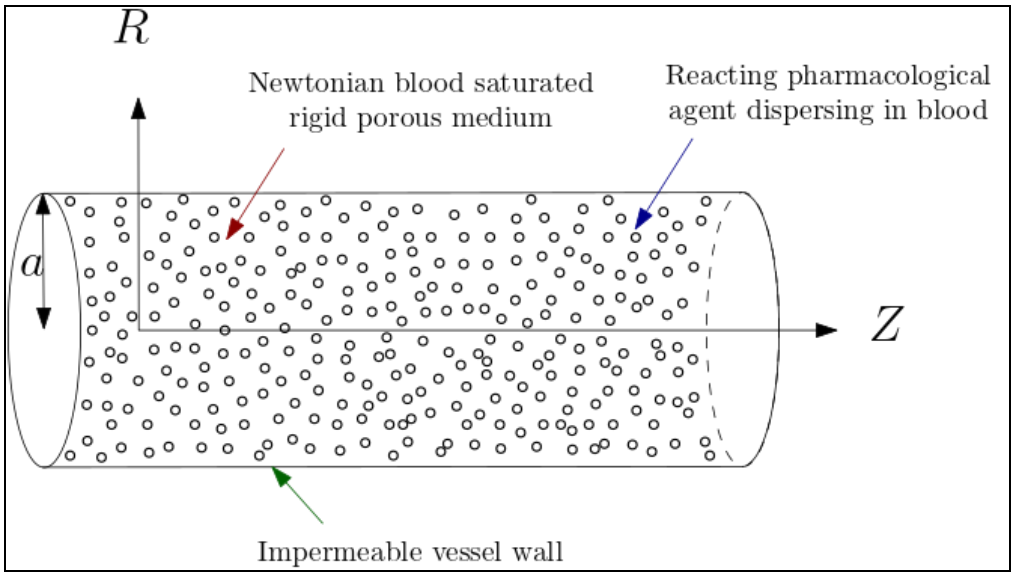

Fig. 1 Schematic diagram of reactive dispersion in Newtonian blood flow in a non-Darcy porous medium vessel

Equation (6) describes the flow velocity equation for saturated porous media and is known as the Brinkman-Forchheimer-Darcy equation. Many studies of fluid flow in porous media are based on Darcy law, but one drawback of this law is that it is applicable only for small Reynolds numbers $(\mathrm{Re} < 1)$. However, there are several cases when the flow velocity is slow with relatively high Reynolds numbers; in such cases, the flow exhibits non-linearity characteristics and cannot be modelled according to Darcy's law. This deficiency can be overcome with the consideration of Brinkman-Forchheimer-Darcy drag force formulation for hydrodynamics of porous media. For the present hemodynamic regime, the transport Eq. (5) reduces to:

$$\frac{\partial C}{\partial t}+\frac{U}{\phi}\frac{\partial C}{\partial Z}=D_L^{\mathrm{eff}}\frac{\partial^2 C}{\partial Z^2}+\frac{D_R^{\mathrm{eff}}}{R}\frac{\partial}{\partial R}\left(R\frac{\partial C}{\partial R}\right)-\beta C,\ 0<R<a. \tag{8}$$

Where, Z and R are respectively axial and radial coordinate. $D_L^{\mathrm{eff}}=k(\lambda+D_L/\phi)$ and $D_r^{\mathrm{eff}}=k(\lambda+D_r/\phi)$ are the longitudinal and transverse diffusion coefficient. The species (solute) of mass M (e. g. drag) is instantaneous release into the blood flow at time $t=0$, i.e.,

$$C(0,R,Z)=\frac{M}{\pi a^2}\delta(Z),\quad 0<\xi<a\,. \tag{9}$$

The boundary of the blood vessel considered in the present study is assumed to be impermeable, i.e.,

$$\frac{\partial C}{\partial R}=0\quad \text{at}\quad R=a, \tag{10}$$

again, owing to symmetry, we have:

$$\frac{\partial C}{\partial R}=0\quad \text{at}\quad R=0. \tag{11}$$

The amount of solute released into the flow is finite, and it follows that as a result, the upstream and downstream condition for solute transport (concentration boundary condition) is imposed as:

$$C(t,R,Z)=\frac{\partial C}{\partial R}=0\quad \text{as}\quad Z\to\pm\infty\,, \tag{12}$$

3. NON-DIMENSIONALISATION OF MODEL

Throughout the remainder of the analysis, the following dimensionless quantities are adopted:

$$\tau=\frac{U_0 t}{a},\quad r=\frac{R}{a},\quad z=\frac{Z}{a},\quad \Omega=\frac{\pi a^3 C}{M},\quad u=\frac{U}{U_0}, \tag{13}$$

$U_0=-(a^2/\mu)\partial p/\partial\eta$ is the reference velocity. Using the scaling as defined in Eqn. (13), the initial-boundary value problem (IBVP) given by Eqs. (6-7) emerges as follows:

$$\frac{1}{r}\frac{d}{dr}\left(r\frac{du}{dr}\right)-\frac{u}{\mathrm{Da}}-\frac{\mathrm{F}}{\sqrt{\mathrm{Da}}}u^2+1=0, \tag{14}$$

$$\left.\begin{aligned} u<\infty\quad &\text{at}\quad r=0,\\ u=0\quad &\text{at}\quad r=1.\end{aligned}\right\} \tag{15}$$

Here $\mathrm{Da} = K / a^2$ is the familiar Darcy number and $\mathrm{F} = C_f U_0 a^2 / \nu\sqrt{K}$ is the Forchheimer number which is the product of drag coefficient, Reynolds number, and the square root of Darcy number. Similarly, the dimensionless form of the convection-diffusion Eq. (8) with associated initial and boundary conditions (9-12) is transformed by virtue of Eq. (13) to:

$$\frac{\partial \Omega}{\partial \tau} + \mathrm{Pe}\, u(r) \frac{\partial \Omega}{\partial z} = \frac{1}{r}\frac{\partial}{\partial r}\left(r \frac{\partial \Omega}{\partial r} \right) + R_D \frac{\partial^2 \Omega}{\partial z^2} - \Gamma \Omega\,, \tag{16}$$

$$\Omega(0, r, z) = \frac{\delta(z)}{\phi}, \quad (0 < r < 1), \tag{17}$$

$$\frac{\partial \Omega}{\partial r} = 0 \quad \text{at} \quad r = 0, \tag{18}$$

$$\frac{\partial \Omega}{\partial r} = 0 \quad \text{at} \quad r = 1, \tag{19}$$

$$\frac{\partial \Omega}{\partial r} = \Omega(t, r, z) = 0, \qquad \text{at } z \to \pm\infty. \tag{20}$$

Here $\Gamma = \beta\, a^2 / D_R^{\mathrm{eff}}$ is the dimensionless bulk reaction rate, $R_D = D_L^{\mathrm{eff}} / D_R^{\mathrm{eff}}$ represents the ratio of *axial and radial diffusion* coefficients and $\mathrm{Pe}(= U_0 a / \phi D_R^{\mathrm{eff}})$ is the effective Péclet number which quantifies the relative contribution of *convection to diffusion* in the porous medium.

4. SUPERFICIAL VELOCITY

4.1. For Large Darcy number

The differential Eq. (14) is highly non-linear due to the presence of the penultimate term on the right-hand side and therefore to extract a solution, it is judicious to adopt a regular perturbation method by taking the perturbation parameter as $\grave{o} = 1/\sqrt{\mathrm{Da}}$. We have

considered the case for which the Darcy number is large (very high permeability), so Eq. (14) assumes the form:

$$\frac{1}{r}\frac{d}{dr}\left(r\frac{du}{dr}\right)-\grave{o}^2u-\grave{o}\mathrm{F}u^2+1=0. \tag{21}$$

Proceeding with the analysis, the velocity field is expanded asymptotically with respect to $\grave{o}$ as follows:

$$u(r)=u_0(r)+\grave{o}u_1(r)+O(\grave{o}^2). \tag{22}$$

Inserting the asymptotic expression of Eq. (22) into Eq. (21) and also in the boundary condition (15), collecting the like powers of $\grave{o}$, the differential equation for u_0 and u_1 is obtained. By solving those equations, we arrive at:

$$u(r)=\frac{1}{4}(1-r^2)+\frac{\mathrm{F}}{\sqrt{\mathrm{Da}}1152}\left[2r^6-9r^4+18r^2-11\right]+O\left(\frac{1}{\mathrm{Da}}\right). \tag{23}$$

4.2. For small Darcy number

In contrast to above subsection if the Darcy number is sufficiently small, i.e., $\grave{o}>>1$, then to solve Eqn. (21), we rearrange the problem by multiplying $\grave{o}^{-2}$ on both sides as:

$$\grave{o}^{-2}\frac{1}{r}\frac{d}{dr}\left(r\frac{du}{dr}\right)-u-\grave{o}^{-1}\mathrm{F}u^2+\grave{o}^{-2}=0. \tag{24}$$

Then the above problem (Eq. (24)) is a singular perturbation problem with $1/\grave{o}$ is a perturbation parameter. It is important to mention here that the boundary layer located near the wall i.e. $r=1$, accordingly the outer solution of the problem became

$$u^{\mathrm{out}}=\grave{o}^{-2}. \tag{25}$$

In order to find the inner solution, we use the transformation $\xi=\grave{o}(1-r)$ and neglecting smaller order terms in Eq. (24) we obtain:

$$\frac{d^2u^{\text{in}}}{d\xi^2} - u^{\text{in}} = 0. \tag{26}$$

The solution of Eq. (25) is

$$u^{\text{in}} = A\exp(-\eta) + B\exp(\eta). \tag{27}$$

Where A and B is the arbitrary constant. Using Prandtl's matching conditions as illustrated by Bush (1992), which is of the form

$$\lim_{r\to 1} u^{\text{out}} = \lim_{\xi\to\infty} u^{\text{in}} \tag{28}$$

leads to $B = 0$ and hence the *composite solution of velocity* with the aid of no slip boundary condition is

$$u = \frac{1-\exp\left(\text{ὸ}\left(r-1\right)\right)}{\text{ὸ}^2}. \tag{29}$$

5. GENERALIZED DISPERSION MODEL

Following Gill (1967), we have decomposed the concentration field as follows:

$$\Omega(\tau, r, z) = \bar{\Omega} + \sum_{i=0}^{\infty} f_i(r,t)\frac{\partial^i \bar{\Omega}}{\partial z^i}, \tag{30}$$

where the over-bar indicates a cross-sectional average and is defined as:

$$\bar{g} = 2\int_0^1 rg\,dr. \tag{31}$$

By assuming that the process of mean concentration $\bar{\Omega}$ is diffusive in nature right from the beginning, then accordingly, the *mean concentration* can be expressed as follows:

$$\frac{\partial \bar{\Omega}}{\partial \tau} = \sum_{i=1}^{\infty} K_i(\tau)\frac{\partial^i \bar{\Omega}}{\partial z^i}, \tag{32}$$

The termed K_1 and K_2 in Eq. (32) are termed as the *advection* and *dispersion* coefficient, respectively. Using Eq. (30) in Eq. (32) in Eq. (16) and after some algebraic manipulation, we obtain the following system of partial differential equations:

$$\frac{\partial f_1}{\partial \tau} = \frac{1}{r}\frac{\partial}{\partial r}\left(r\frac{\partial f_1}{\partial r}\right) - \Gamma f_1 - \left(\mathbf{Pe}u + K_1\right), \tag{33}$$

$$\frac{\partial f_2}{\partial \tau} = \frac{1}{r}\frac{\partial}{\partial r}\left(r\frac{\partial f_2}{\partial r}\right) - \Gamma f_2 - \left(\mathbf{Pe}u + K_1\right) f_1 + (R_D - K_2) \tag{34}$$

$$\begin{aligned}\frac{\partial f_{k+2}}{\partial \tau} = \frac{1}{r}\frac{\partial}{\partial r}\left(r\frac{\partial f_{k+2}}{\partial r}\right) - \Gamma f_{k+2} - \left(\mathbf{Pe}u + K_1\right) f_{k+1} + (R_D - K_2) f_k \\ - \sum_{i=3}^{k+2} K_i f_{k+i-2} \quad (k = 1,2,\mathrm{L}\,)\end{aligned} \tag{35}$$

The initial and boundary conditions on $f_k^{'s}$ are prescribed as follows:

$$f_i(0,r) = \delta_{0i}, \qquad (i = 0,1,2) \tag{36}$$

$$\frac{\partial f_i}{\partial r} = 0 \quad (i = 0,1,2) \quad \text{at} \quad r = 1, \tag{37}$$

$$\frac{\partial f_i}{\partial r} = 0, \quad (i = 0,1,2) \quad \text{at} \quad r = 0, \tag{38}$$

Again from Eq. (31) it may be inferred that:

$$\int_0^1 r \cdot f_i(r,t)dr = 0 \tag{39}$$

The coefficients K_1 and K_2 can be derived by taking the cross-sectional average of Eq. (16) as:

$$K_1(\tau) = -\mathrm{Pe}\bar{u}, \tag{40}$$

$$K_2(\tau) = R_D - 2\mathrm{Pe}\int_0^1 r f_1 u dr. \tag{41}$$

$$K_{i+2}(\tau) = -2\mathrm{Pe}\int_0^1 r f_{i+1} u dr. \tag{42}$$

5.1. Dispersion coefficient:

To obtain the solution of Eqn. (33) we have decomposed f_1 into two parts as follows:

$$f_1(r,\tau) = f_{1s}(r) + f_{1\tau}(r,\tau) \tag{43}$$

The function $f_{1\tau}(r,\tau)$ is the *transient* part of the solution and tends to zero with the progress of time. Therefore, the differential equations for f_{1s} and $f_{1\tau}$ are respectively:

$$\frac{1}{r}\frac{d}{dr}\left(r\frac{df_{1s}}{dr}\right) - \Gamma f_{1s} = \mathrm{Pe}\left(u - \bar{u}\right), \tag{44}$$

$$\frac{\partial f_{1\tau}}{\partial \tau} = \frac{1}{r}\frac{\partial}{\partial r}\left(r\frac{\partial f_{1\tau}}{\partial r}\right) - \Gamma f_{1\tau}, \tag{45}$$

With,

$$f_{1\tau}(0,r) = -f_{1s}(r), \tag{46}$$

$$\frac{\partial f_{1s}}{\partial r} = 0 \qquad \text{at} \quad r = 0,1, \tag{47}$$

$$\frac{\partial f_{1\tau}}{\partial r} = 0 \quad \text{at} \quad r = 0,1. \tag{48}$$

Eq. (39) becomes:

$$\int_0^1 r \cdot f_{1s}(r)dr = \int_0^1 r \cdot f_{1\tau}(r,t)dr = 0. \tag{49}$$

The solution of Eqns. (44) (for large Darcy velocity) and (45) subject to boundary conditions (46-48) are as follows:

$$f_{1s}(r) = A_1 J_0(\alpha r) + b(r), \tag{50}$$

Here:

$$A_1 = \frac{Pe\left(192F\varepsilon + F\varepsilon\alpha^4 - 48\alpha^4\right)}{96\alpha^7 I_1(\alpha)}, \tag{51}$$

$$b(r)=\frac{\mathrm{Pe}}{4\alpha^4}\left\{\alpha^2r^2+4-\alpha^2+4\bar{u}\alpha^2\right\}+\frac{\mathrm{FPe}}{1152\sqrt{\mathrm{Da}}\alpha^8}\left\{-2\alpha^6r^6+\left(9\alpha^6-72\alpha^4\right)r^4\right.$$
$$\left.+\left(-18\alpha^6+144\alpha^4-1152\alpha^2\right)r^2-\left(4608-11\alpha^6+72\alpha^4-576\alpha^2\right)\right\}, \quad (52)$$

and

$$f_{1\tau}(r,\tau)=\sum_{n=1}^{\infty}B_nJ_0(\mu_nr)\exp(-\alpha^2\tau-\mu_n^2\tau), \quad (53)$$

where,

$$B_n=-\frac{2\int_0^1 rf_{1s}(r)J_0(\mu_nr)dr}{J_0^2(\mu_n)}. \quad (54)$$

Here $\alpha^2=\Gamma$ and μ_n is the *positive* root of the Bessel function $J_1(x)=0$. If $\alpha\to 0$ then the solutions are given by Eqns. (49) and (52) emerge as:

$$\lim_{\alpha\to 0} f_{1s}(r)=-\frac{Pe}{192}\left(3r^4-6r^2+2\right)+\frac{F\mathrm{Pe}}{36864\sqrt{\mathrm{Da}}}\left(r^8-8r^6+36r^4-52r^2+\frac{79}{5}\right) \quad (55)$$

$$\lim_{\alpha\to 0} f_{1\tau}(r)=\sum_{n=1}^{\infty}B_nJ_0(\mu_nr)e^{-\mu_n^2\tau} \quad (56)$$

Accordingly, From Eq. (41) we get the dispersion coefficient *with reaction and without reaction for large Darcy number*. To solve the Eq. (44) analytically for small Darcy number is difficult due to the presence of exponential function in the right side of the differential Eq. (44), thus we have adopted the Crank Nicolson implicit scheme to get the solution. Additionally, due to bulk degradation, the rate of decrease is further assessed by defining $R_{K_2,\alpha}$ as:

$$R_{K_2,\alpha}=1-\frac{K_2}{K_2\big|_{\alpha=0}} \quad (57)$$

Here $K_2\big|_{\alpha=0}$ is the dispersion coefficient *without reaction for an isotopic solution* $\left(R_D=1\right)$.

2.3-2 Mean and Transverse Concentration

The expression for the higher-order term in the series solutions defined by Eqns. (30) and (32) are negligible (Wang and Chen, 2016) and at the large time $\tau \geq 3$ only $f_0(r,\tau)$ is sufficient to estimate the solute concentration. Therefore, by neglecting the K_3 onwards from Eqn. (32) we get:

$$\frac{\partial \bar{\Omega}}{\partial \tau} = -\mathrm{Pe}\bar{u}\frac{\partial \bar{\Omega}}{\partial z} + K_2(\tau)\frac{\partial^2 \bar{\Omega}}{\partial z^2}. \tag{58}$$

The solution of Eq. (58) is w.r.t. the initial boundary condition given earlier is:

$$\bar{\Omega} = \frac{1}{2\phi\sqrt{\pi\xi(\tau)}}\exp\left(-\frac{\left(z-\mathrm{Pe}\bar{u}\tau\right)^2}{4\xi(\tau)}\right), \tag{59}$$

where,

$$\xi(\tau) = \int_0^{\tau} K_2(s)ds. \tag{60}$$

The transverse concentration is obtained from Eqn. (30) as:

$$\Omega(\tau,r,z) = \bar{\Omega} + \sum_{i=0}^{\infty} f_i(r,t)\frac{\partial^i \bar{\Omega}}{\partial z^i} \tag{61}$$

However, with the progress of time, the higher-order terms of the series become negligible. Wang and Chen (2016) have shown that after time $\tau \geq 3$, only the first term of the series is sufficient i.e.:

$$\Omega(\tau,r,z) = \bar{\Omega} + f_1(r,t)\frac{\partial \bar{\Omega}}{\partial z} \tag{62}$$

6. RESULTS AND DISCUSSION

Evidently, significant suppression in radial velocity accompanies a rise in F. The symmetric boundary conditions at the wall ensure that symmetric parabolic distributions are obtained across the vessel cross-section i.e., $-1 \leq r \leq 1$. Although greater F implies increasing inertial contribution in the flow, the overwhelming effect of quadratic drag is

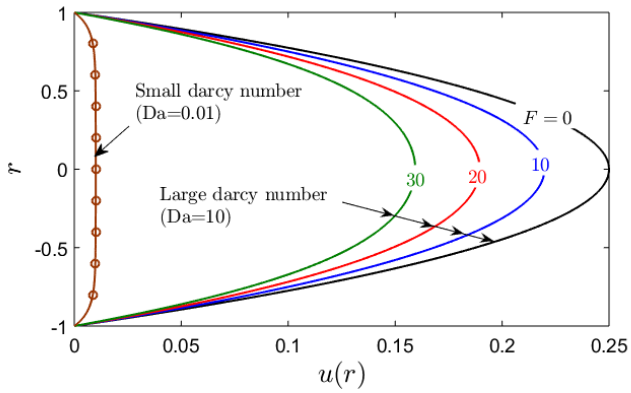

Fig 2. Dimensionless velocity distribution for a variety of Forchheimer number for small and large darcy number.

the deceleration of the blood flow in the porous regime. This is characteristic of Forchheimer's effects and has been computed in numerous other studies, including Vafai and Tien (1982) and Dybbs and Edwards (1984). It is noteworthy that the purely fluid regime scenario can be recovered for $\mathrm{Da} \to \infty$ and $\mathrm{F} = 0$. The Darcy drag force consequence of the viscous contribution to stress at the solid particle boundaries. As such, with increasing permeability , the flow becomes gradually less sensitive to porous fibers, which decrease in concentration. Inertial effects due to the porous medium are experienced via the quadratic drag term i.e., Forchheimer term, which does not directly include viscosity but arises through the action of viscosity, caused by the inertial effects propagation of pressure distribution which also contributes to the stress at the rigid boundary of the vessel surface. Forchheimer drag, as shown by Joseph et al. (1982) models, basically a form drag phenomenon, which in reality involves the separation of boundary layers and creation of wake next to solid impediments (solid matrix fibers, bundles, etc.). The pore-scale convective inertial effects contributing to the form drag results in a significant change of the velocity field and intensify in the macroscopic region where the gradient of pore-scale velocity are high. Lage (1998) has clearly demonstrated

that these characteristics are applicable to both bluff body type porous media as well as those of the conduit type (relevant to the present model). Skjetne and Auriault (1999) has further observed a strong inertial flow regime in porous media due to the Forchheimer drag. This refers to the flow regime where the pore Reynolds number, Re (which depends on particle or pore diameter), is approximately greater or equal to unity, and the model deviates from the traditional porous media transport physics (purely Darcian or viscous-dominated). It is also pertinent to note that the range of F values considered up to 30 does not stimulate vortex formation associated with higher Reynolds numbers (greater than 250). However, the boundary layers around the pores become more prominent, and an "inertial core" can be seen with a higher Forchheimer number, and creation of such "core" is accountable for the non-linear relationship between flow rate and the pressure drop.

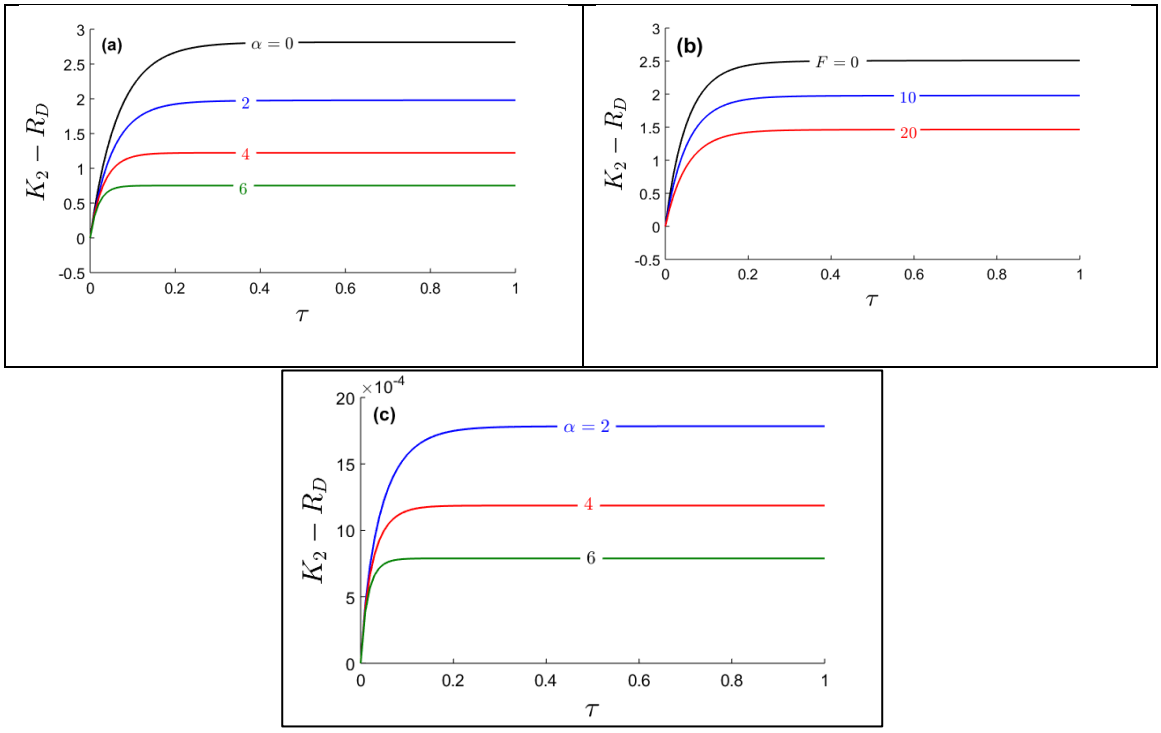

Fig 3. Plots of $K_2 - R_D$; (a) for a variety of reaction parameters for large Darcy number ($\mathrm{Da} = 10$, $\mathrm{Pe} = 100$, and $F = 10$); (b) for a variety of Forchheimer numbers large Darcy number ($\mathrm{Da} = 10$, $\mathrm{Pe} = 100$, and $\alpha = 1$); (c) for a variety of reaction parameters for small Darcy number ($\mathrm{Da} = 0.01$, and $\mathrm{Pe} = 100$).

Figures 3 and 4 are presented in order to analyze the dispersion coefficient (from which the ratio of axial diffusion to radial diffusion). **Figures** 3a, b visualize the time-dependent behavior for a variety of reaction parameters and also Forchheimer numbers. This behaviour is induced due to the reaction involved in the present blood flow, while the second one is associated with velocity, however, in all cases the dispersion coefficient ultimately reaches their steady state (Debnath et al., 2017a,b). **Figure** 3(a) shows that an increase in the reaction parameter decreases the dispersion coefficient. This is attributable to the fact that the number of moles involved in the reaction often increases with the increase of the reaction rate, and as a consequence dispersion coefficient is reduced (Debnath and Ghoshal, 2020; Debnath et al., 2019a; Roy et al., 2017). The same decreasing nature of the dispersion coefficient is also induced with increasing Forchheimer number (**Fig.** 3(b)), and this is probably associated with the deceleration (retardation) in axial flow with greater quadratic drag effect. Although both the parameters are responsible for decreasing the effective dispersion coefficient, they exert a different modification in the topology of profiles (**Figs.** 4a,b). With the increment in Forchheimer number, the dispersion coefficient decays linearly; however, this is not the case for greater reaction parameters.

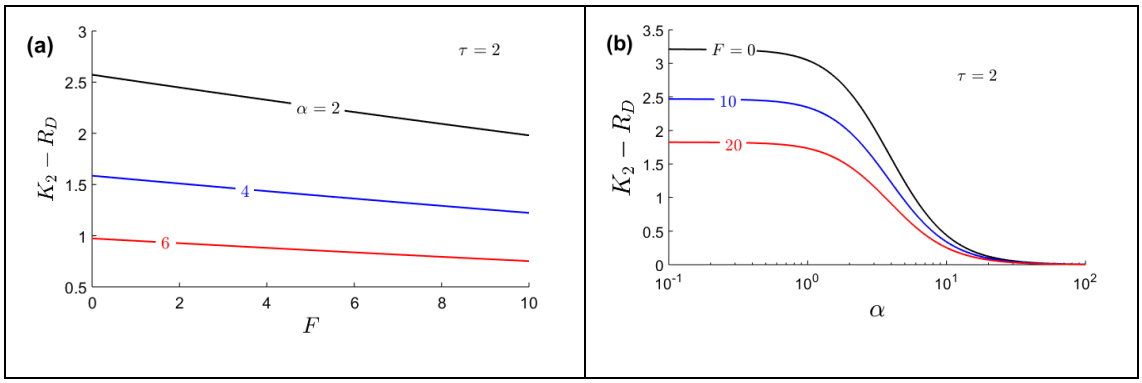

Fig 4. Asymptotic dispersion coefficient $(K_2 - R_D)$ with (a) Forchheimer number and (b) bulk reaction parameter where ($\mathrm{Da} = 10$ and $\mathrm{Pe} = 100$) .

The reduction rate is initially steady with increasing reaction parameters; subsequently, a sharp increase is observed in the reduction rate. However, this transition does not exist for large reaction parameters (**Fig**. 5). It is important to note that the initial steady reduction rate varies with the chemical reaction parameter and can be controlled by Forchheimer number i.e., quadratic drag effect.

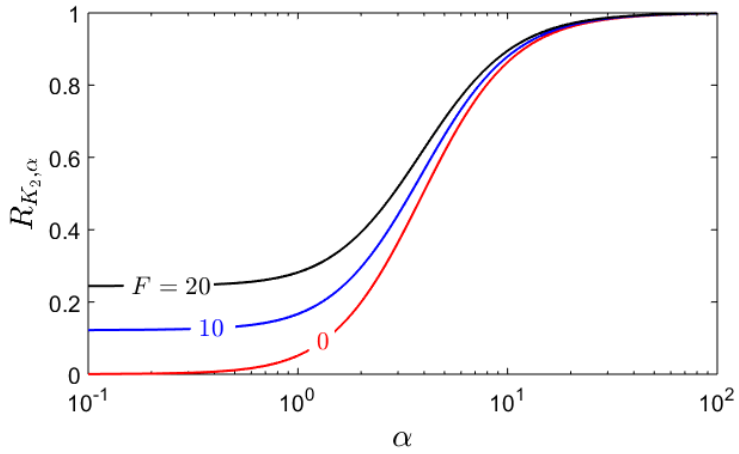

Fig 5. Variation of $R_{K_2,\alpha}$ with α at asymptotic time $\tau = 2$ $\mathrm{Da} = 10$ where ($\mathrm{Da} = 10$ and $\mathrm{Pe} = 100$).

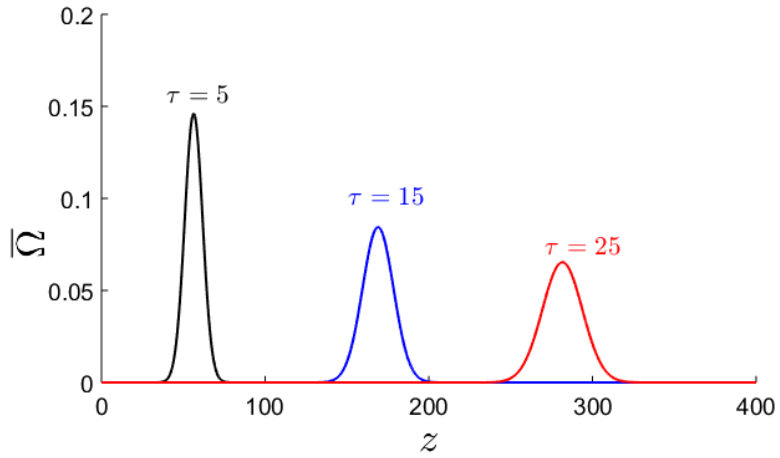

Fig 6. Mean concentration with axial distance at different dimensionless times where $\mathrm{Da} = 10$, $F = 10$, $\phi = 0.5$, $R_D = 1$ and $\mathrm{Pe} = 100$.

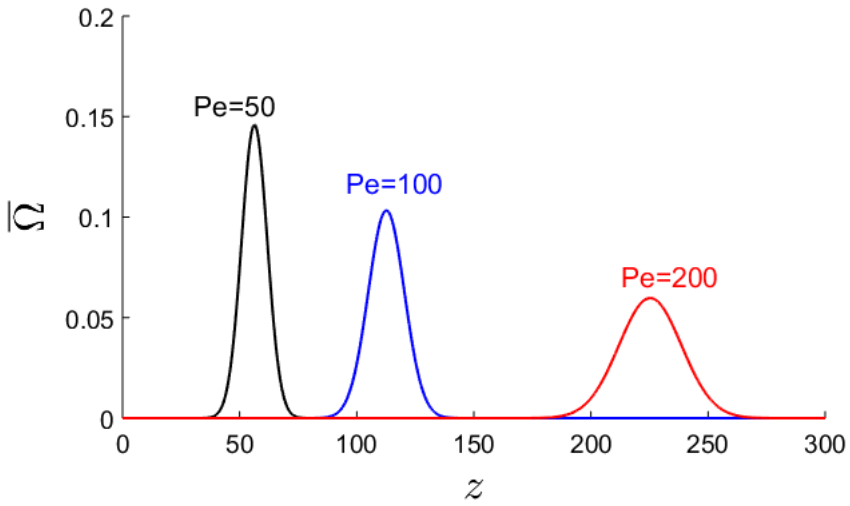

Fig 7. Mean concentration with axial distance at different Péclet numbers where $\mathrm{Da}=10$, $F=10$, $\phi=0.5$, $R_D=1$ and $\tau=10$.

Figure 6 illustrates how the centroid of the solute cloud is propagated into the downstream region of the blood vessel. The figure also reveals that the peak of the mean concentration deteriorates over time. This is induced since the dispersion process is largely controlled by diffusion at large times, and therefore the breakthrough curve is more evenly dispersed. A similar trend is additionally computed with a greater effective Péclet number. A large Péclet number means the process is *diffusion-controlled* (**Fig**. 7). **Figure** 8a shows that the peak of the mean concentration increases with Forchheimer number; however, the central location of the solute (pharmacological agent) cloud is displaced in the backward direction; the decrease in mean velocity with Forchheimer number generates this migration. In contrast to **Fig**. 8(a) other figures (**Fig**. 8b,c,d) show that the peak of the mean concentration decrease with reaction parameter (Debnath et al., 2019b; Roy et al., 2019), porosity and R_D, and furthermore, that the centroid of the solute cloud remains unchanged.

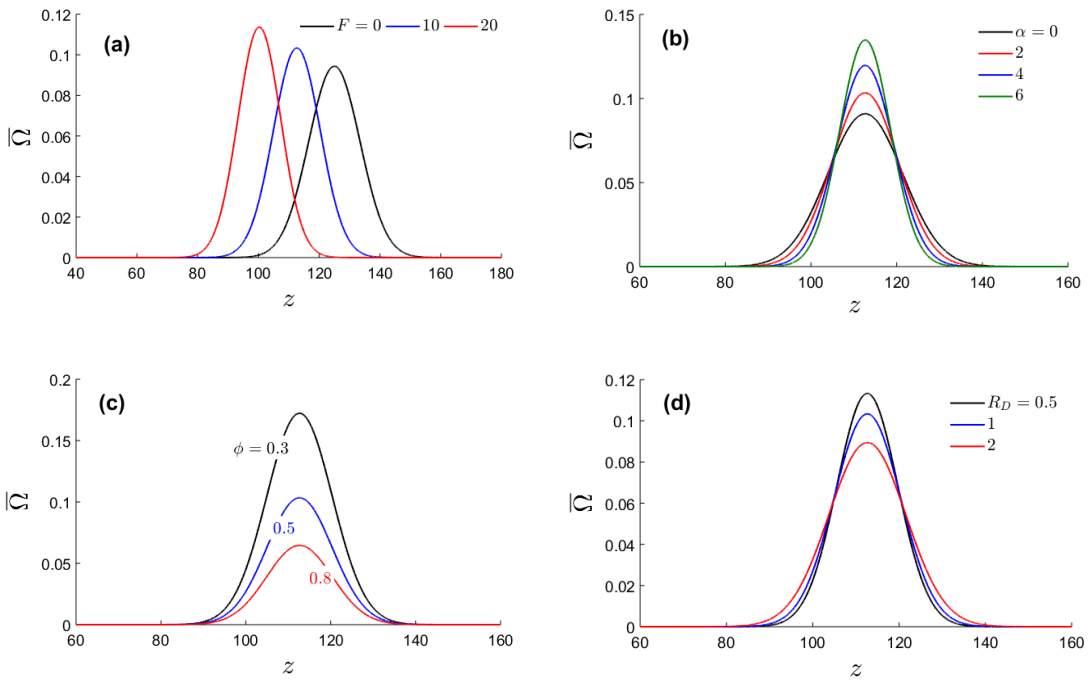

Fig 8. Axial mean concentration at the dimensionless time $\tau = 10$ with $\mathrm{Da} = 10$ and $\mathrm{Pe} = 100$; (a) for variety of Forchheimer number ($\phi = 0.5$, $\alpha = 2$, and $R_D = 1$) (b) for variety of reaction parameter ($\phi = 0.5$, $F = 10$, and $R_D = 1$) (c) for variety of Porosity ($F = 10$, $\alpha = 2$, and $R_D = 1$) (d) for variety of diffusion ratios ($\phi = 0.5$, $\alpha = 2$, and $F = 10$).

Using Eq. (56) several graphs are also presented for the transverse variation of the concentration in upstream and downstream at different times with a variation in bulk reaction parameter (α). **Figures** 9(a-d) show that with a change in axial location, there is a substantial alteration in profiles which morph from smooth ascents at $\eta = -0.1$ to decays at $\eta = 0.1$ (for both times of $\tau = 5$ and 10). The axial location $\eta (= z - \mathrm{Pe}\bar{u}\tau)$ is measures from center of gravity of the injected solute which is moving with the average velocity of the blood. The topology in transverse concentration is therefore sustained with time but modified with the axial location. Generally, transverse concentration is significantly elevated with increasing bulk reaction parameter (α), at all radial and axial locations, and at all time instants.

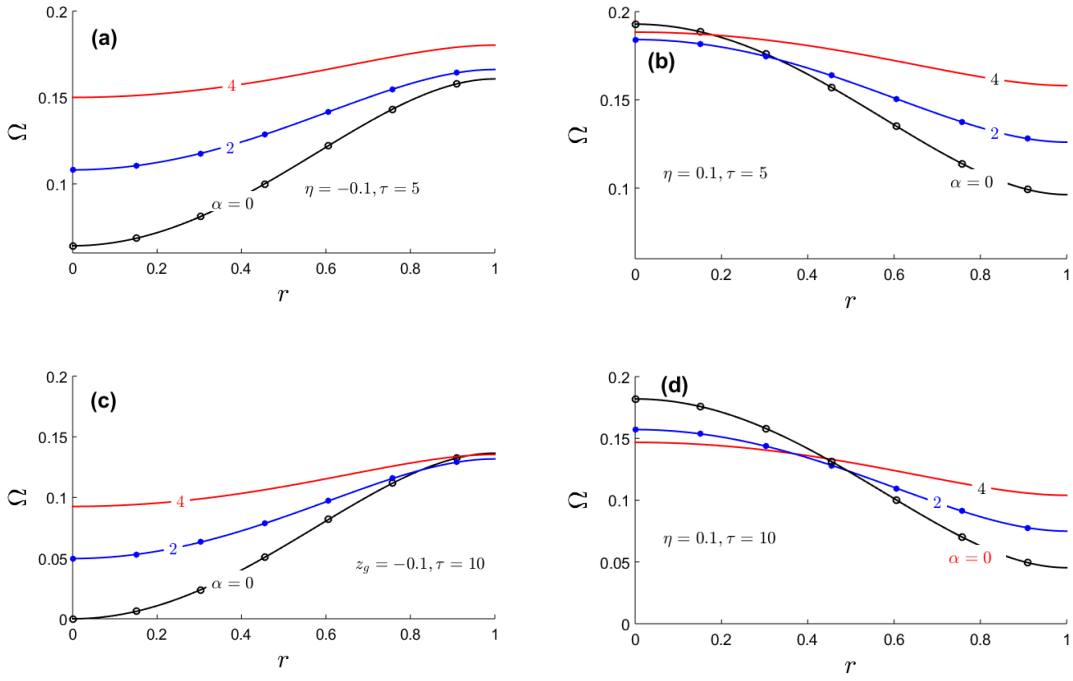

Fig 9. Transverse concentration at different axial location and different times for various bulk reaction parameters, α but fixed $\phi = 0.5$, $F = 10, \mathrm{Pe} = 100, \mathrm{Da} = 10$ and $R_D = 1$.

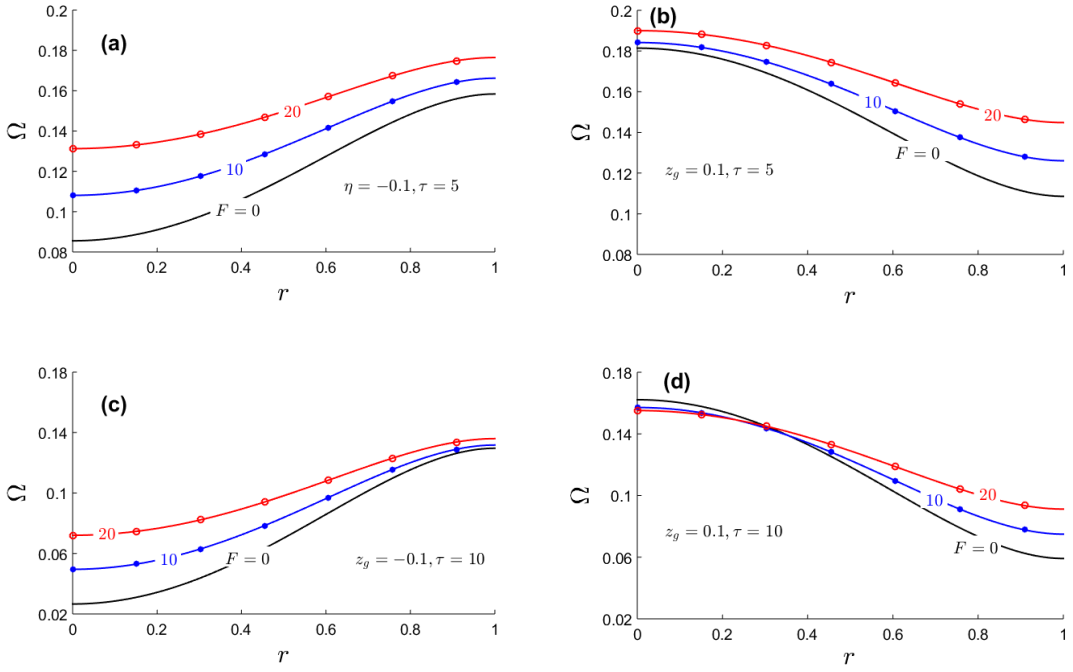

Fig 10. Transverse concentration at different axial location and different times for various Forchheimer numbers, F where, $\phi = 0.5, \alpha = 2, \mathrm{Pe} = 100, \mathrm{Da} = 10$ and $R_D = 1$.

Figures 10(a-d) indicate that with a change in axial location, there is again a marked alteration in profiles which morph from smooth ascents at $z = -0.1$ to decays at $z = 0.1$

(for both times of $\tau = 5$ and 10). Increasing Forchheimer number strongly boosts the transverse concentration magnitudes at all radial locations. Transverse concentration is therefore minimized for the Darcian case $(\mathrm{F} = 0)$ and maximized for the strongly quadratic drag case $(\mathrm{F} = 20)$. Inertial drag, therefore, encourages transverse diffusion.

7.CONCLUSIONS

A comprehensive mathematical model has been developed for solute transport in unsteady blood flow through a rigid, impermeable blood vessel containing a non-Darcy porous medium, as a model for drug movement (pharmaco-dynamics) in blood vessels containing fatty deposits. The Darcy-Brinkman-Forchheimer drag force formulation is adopted to mimic a sparsely packed porous domain, and the vessel is approximated as an impermeable cylindrical conduit. The conservation equations are formulated in an axisymmetric system (R, Z) with appropriate boundary conditions, assuming constant tortuosity and porosity of the medium. Newtonian flow is assumed, which is physically realistic for large vessels at high shear rates. Both axial and radial diffusion are considered. The general governing equation of the blood flow is then non-dimensionalized and solved using a regular perturbation method taking the perturbation parameter as $1/\sqrt{\mathrm{Da}}$ where Da is the Darcy number (dimensionless permeability parameter). The velocity field is expanded asymptotically, and the concentration field decomposed. Advection and dispersion coefficient expressions are rigorously derived. Extensive visualization of the influence of effective Péclet number, Forchheimer number, reaction parameter on velocity, asymptotic dispersion coefficient, mean concentration, the transverse concentration at different axial locations and times, is provided. The present computations have shown that:

(I) Increasing reaction parameter and Forchheimer number both decrease the dispersion coefficient, although the latter exhibits a linear decay.

(II) The maximum mean concentration is enhanced with greater Forchheimer numbers, although the centre of the solute cloud is displaced in the backward direction.

(III) Peak mean concentration is suppressed with the reaction parameter, although the centroid of the solute cloud remains unchanged.

(IV) Peak mean concentration deteriorates over time since the dispersion process is mostly controlled by diffusion at the large time, and therefore the breakthrough curve is more dispersed. A similar trend is computed with increasing P\'eclet numbers (large Péclet numbers imply diffusion-controlled transport).

(V) Transverse concentration is significantly elevated with increasing bulk reaction parameter (α), at all radial and axial locations, and at all time instants.

(VI) Increasing Forchheimer number strongly boosts the transverse concentration magnitudes at all radial locations and is minimized for the Darcian case $(F = 0)$

The computations provide some insight into drugs (pharmacological agents) reacting linearly with blood. However, attention has been confined to Newtonian flow. Future studies may explore non-Newtonian models for hemorheological characteristics e.g., viscoelastic (Dubey et al., 2020), and will be communicated imminently.

ACKNOWLEDGEMENTS:

The authors wish to thank Prof. Pradeep. G. Siddheshwar for his excellent advice in the development of the mathematical model. All the authors also appreciate the helpful comments of the reviewers which have improved the manuscript in clarity.

Conflict of interest

The authors declare that they have no conflict of interest.

REFERENCES:

Beavers, G.S., Sparrow, E.M., Magnuson, R.A.: Experiments on coupled parallel flows in a channel and a bounding porous medium. ASME J. Basic Eng. **92**, 843–848(1970)

Bég, O.A., Bhargava R., Rawat S., Halim K., Takhar HS: Computational modeling of biomagnetic micropolar blood flow and heat transfer in a two-dimensional non-Darcian porous medium. Meccanica **43**(4), 391–410(2007)

Bég, O.A., Bég T.A., Bhargava, R., Rawat, S., Tripathi, D.: Finite element study of pulsatile magneto-hemodynamic non-Newtonian flow and drug diffusion in a porous medium channel. J. Mech. Med. Biol. **12**(04), 1250081(2012)

Bég, O.A., Rashidi, M.M., Rahimzadeh, N., Bég, T.A., Hung, T.K.: Homotopy Simulation of two-phase thermo-hemodynamic filtration in a high permeability blood purification device. J. Mech. Med. Biol. **13**(04), 1350066(2013)

Brinkman, H.C.: A calculation of the viscous force exerted by a flowing fluid on a dense swarm of particles. Flow Turbul. Combust. **1**(1), 27(1949).

Brinkman, H.C.: On the permeability of media consisting of closely packed porous particles. Flow Turbul. Combust. **1**(1), 81(1949)

Brinkman, H.C.: Problems of fluid flow through swarms of particles and through macromolecules in solution. Research; a journal of science and its application **2**(4), 190–194(1949)

Bush, A.W.: Perturbation Methods for Engineers and Scientists. CRC Press, Boca Raton (1992)

Chapelle D., Gerbeau J.F., Sainte-Marie J., Vignon-Clementel I.E.: A poroelastic model valid in large strains with applications to perfusion in cardiac modeling. Comput. Mech. **46**(1), 91–101(2009)

Chen G.Q., Wu Z.: Taylor dispersion in a two-zone packed tube. Int. J. Heat Mass Transfer **55**(1-3), 43–52(2012) Chen, G.Q., Zeng, L.: Taylor dispersion in a packed tube. Commun. Nonlinear Sci. Numer. Simul. **14**(5), 2215–2221(2009)

Dash, R.K., Mehta, K.N., Jayaraman, G.: Effect of yield stress on the flow of a Casson fluid in a homogeneous porous medium bounded by a circular tube. Appl. Sci. Res. **57**(2), 133–149(1996)

Debnath, S., Ghoshal, K.: Transport of reactive species in oscillatory Couette-Poiseuille flows subject to homogeneous and heterogeneous reactions. Appl. Math. Comput. **385**, 125387(2020)

Debnath, S., Saha, A.K., Mazumder, B.S., Roy, A.K.: Dispersion phenomena of reactive solute in a pulsatile flow of three-layer liquids. Phys. Fluids **29**(9), 097107(2017)

Debnath, S., Saha, A.K., Mazumder, B.S., Roy, A.K.: Hydrodynamic dispersion of reactive solute in a Hagen–Poiseuille flow of a layered liquid. Chin. J. Chem. Eng. **25**(7), 862–873(2017)

Debnath S., Saha A.K., Mazumder B.S., Roy A.K.: On transport of reactive solute in a pulsatile Casson fluid flow through an annulus. Int. J. Comput. Math, 1–17(2019)

Debnath, S., Saha, A.K., Mazumder, B.S., Roy, A.K.: Transport of a reactive solute in a pulsatile non-Newtonian liquid flowing through an annular pipe. J. Eng. Math. **116**(1), 1–22(2019).

Dubey, A., Vasu, B., Bég, O.A., Gorla R.S.R., Kadir A.: Computational fluid dynamic simulation of two-fluid non-Newtonian nanohemodynamics through a diseased artery with a stenosis and aneurysm. Comput. Methods Biomech. Biomed. Eng. **23**(8), 345–371, (2020)

Dybbs, A., Edwards, R.V.: A new look at porous media fluid mechanics Darcy to turbulent. Bear, J. and Corapcioglu, M.Y. Fundamentals of transport phenomena in porous media. pp. 199–256(1984)

Gill, W.N.: A note on the solution of transient dispersion problems. Proc. R. Soc. Lond. A Math. Phys. Sci. **298**(1454), 335–339(1967)

Joseph, D.D., Nield, D.A., Papanicolaou G.: Nonlinear equation governing flow in a saturated porous medium. Water Resour. Res. **18**(4), 1049–1052(1982)

Lage, J.: The fundamental theory of flow through permeable media from Darcy to turbulence. Ingham, D.B and Pop. I.(eds.) Transport phenomena in porous media. pp. 1–31 (1998)

Lake, L.W.: Enhanced Oil Recovery. Prentice Hall Inc., United States (1989)

Lapwood E.R.: Convection of a fluid in a porous medium. Proc. Cambridge Phil. Soc., **44**, 508–521(1948)

Lundgren, T.S.: Slow flow through stationary random beds and suspensions of spheres. J. Fluid Mech. **51**(2), 273–299(1972)

Mueller, C.F., Laude, K., McNally, J.S., Harrison D.G.: Redox mechanisms in blood vessels. Arterioscler Thromb. Vasc. Biol. **25**(2), 274–278(2005)

Nield, DA, Bejan, A (2013) Forced Convection, vol 3. Springer

Ohara, Y., Peterson, T.E., Harrison, D.G.: Hypercholesterolemia increases endothelial superoxide anion production. J. Clin. Invest. **91**(6), 2546–2551(1993)

Ortega, J.M.: A porous media model for blood flow within reticulated foam. Chem. Eng. Sci. **99**, 59–66,(2013)

Peppas, N.A., Sahlin, J.J.: A simple equation for the description of solute release. III. coupling of diffusion and relaxation. Int. J. Pharm. **57**(2), 169–172(1989)

Popova, O.H., Small, M.J., McCoy, S.T., Thomas A.C., Karimi B., Goodman A., Carter K.M.: Comparative analysis of carbon dioxide storage resource assessment methodologies. Environ. Geosci. **19**(3), 105–124(2012)

Rashidi, M.M., Keimanesh, M., Bég, O.A., Hung, T.K.: Magnetohydrodynamic biorheological transport phenomena in a porous medium: a simulation of magnetic blood flow control and filtration. Int. J. Numer. Methods Biomed. Eng. **27**(6), 805–821

Ravi Kiran, G., Radhakrishnamacharya, G., Bég, O.A.: Peristaltic flow and hydrodynamic dispersion of a reactive micropolar fluid-simulation of chemical effects in the digestive process. J. Mech. Med. Biol. **17**(01), 1750013(2017)

Roy, A.K., Saha, A.K., Debnath, S.: On dispersion in oscillatory annular flow driven jointly by pressure pulsation and wall oscillation. J. Appl. Fluid. Mech. **10**(5), 1487–1500(2017)

Roy, A.K., Saha, A.K., Debnath, S.: Hydrodynamic dispersion of solute under homogeneous and heterogeneous reactions. Int. J. Heat Technol. **37**(2), 387–397(2019)

Saffman, P.G.: A theory of dispersion in a porous medium. J. Fluid Mech. **6**(3), 321–349(1959).

Saffman, P.G.: On the boundary condition at the surface of a porous medium. Stud. Appl. Math. **50**(2), 93–101 (1971) .

Sahimi, M.: Flow and Transport in Porous Media and Fractured Rock. John Wiley & Sons, (2011).

Saltzman, W.M.: Drug delivery: engineering principles for drug therapy. Oxford University Press, (2001).

Skjetne E., Auriault J.: New insights on steady, non-linear flow in porous media. Eur. J. Mech. B. Fluids **18**(1), 131–145(1999)

Slattery, J.C.: Flow of viscoelastic fluids through porous media. AIChE J. **13**(6), 1066–1071(1967)

Slattery, J.C.: Two-phase flow through porous media. AIChE J. **16**(3), 345–352 (1970)

Srivastava V., Tripathi D., Bég O.A.: Numerical study of oxygen diffusion from capillary to tissues during hypoxia with external force effects. J. Mech. Med. Biol. **17**(02), 1750027, (2017)

Szulczewski, M.L., MacMinn, C.W., Herzog, H.J., Juanes, R.: Lifetime of carbon capture and storage as a climate-change mitigation technology. Proc. Natl. Acad. Sci. **109**(14), 5185–5189(2012)

Tam, C.K.W.: The drag on a cloud of spherical particles in low Reynolds number flow. J. Fluid Mech. **38**(3),537–546(1969)

Taniyama, Y., Griendling, K.K.: Reactive oxygen species in the vasculature: molecular and cellular mechanisms. Hypertension **42**(6), 1075–1081(2003)

Taylor, G.: Dispersion of soluble matter in solvent flowing slowly through a tube. Proc. R. Soc. Lond. A Math. Phys. Sci. **219**(1137), 186–203(1953)

Touyz, R.M., Schiffrin E.L.: Reactive oxygen species in vascular biology: implications in hypertension. Histochem. Cell Biol. **122**(4), 339–352(2004)

Tripathi, D., Bég, O.A., Curiel-Sosa, J.L.: Homotopy semi-numerical simulation of peristaltic flow of generalised Oldroyd-B fluids with slip effects. Comput. Methods Biomech. Biomed. Eng. **17**(4), 433–442(2012)

Tripathi, D., Bég, O.A.: A numerical study of oscillating peristaltic flow of generalized Maxwell viscoelastic fluids through a porous medium. Transp. Porous Media **95**(2), 337–348(2012)

Tripathi, D., Bég, O.A.: Magnetohydrodynamic peristaltic flow of a couple stress fluid through coaxial channels containing a porous medium. J. Mech. Med. Biol. **12**(05), 1250088(2012)

Tripathi, J., Vasu, B., Dubey, A., Gorla, R.S.R., Murthy, P.V.S.N., Bég, O.A., Saikrishnan, P.: A review on recent advancements in the hemodynamics of nano-drug delivery systems. Nanoscience and Technology: An International Journal **11**(1), 73–98(2020)

Vafai, K., Kim, S.J.: On the limitations of the Brinkman-Forchheimer-extended Darcy equation. Int. J. Heat Fluid Flow **16**(1), 11–15(1995)

Vafai, K., Tien, C.: Boundary and inertia effects on convective mass transfer in porous media. Int. J. Heat Mass Transfer **25**(8), 1183–1190(1982)

Wang P., Chen G.Q.: Environmental dispersion in a tidal wetland with sorption by vegetation. Commun. Nonlinear Sci. Numer. Simul. **22**(1-3), 348–366(2015)

Wang, P., Chen, G.Q.: Transverse concentration distribution in Taylor dispersion: Gill's method of series expansion supported by concentration moments. Int. J. Heat Mass Transfer **95**, 131–141(2016).

Wang, P., Wu, Z., Chen, G.Q., Cui, B.S.: Environmental dispersion in a three-layer wetland flow with free-surface. Commun. Nonlinear Sci. Numer. Simul. **18**(12), 3382–3406(2013)

Wang, P., Li, Z., Wu, X., An, Y.: Taylor dispersion in a packed pipe with wall reaction: Based on the method of Gill's series solution. Int. J. Heat Mass Transfer **91**, 89–97(2015)

Weiser, J.R., Saltzman, W.M.: Controlled release for local delivery of drugs: barriers and models. J. Controlled Release **190**, 664–673(2014).

Whitaker, S.: Diffusion and dispersion in porous media. AIChE J. **13**(3), 420–427(1967).